



## *Supplement of*

# **Impact of the ice thickness distribution discretization on the sea ice concentration variability in the NEMO3.6–LIM3 global ocean–sea ice model**

**Eduardo Moreno-Chamarro et al.**

*Correspondence to:* Eduardo Moreno-Chamarro ([eduardo.moreno@bsc.es](mailto:eduardo.moreno@bsc.es))

The copyright of individual parts of the supplement might differ from the CC BY 4.0 License.

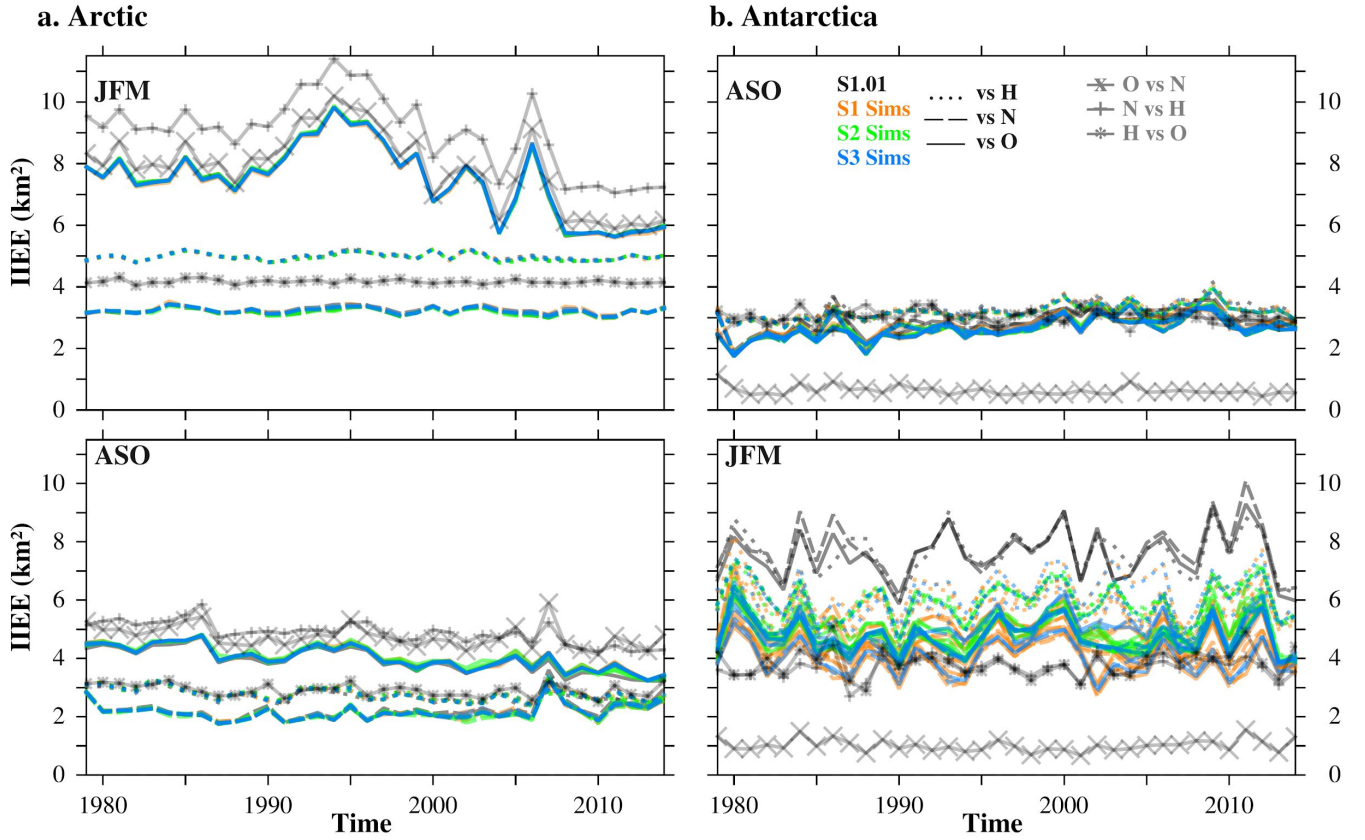


**Fig. S1:** (a) Arctic and (b) Antarctic integrated ice edge error (IIEE; in km<sup>2</sup>) between the simulated SIC in the S1 (red lines), S2 (green lines), and S3 (blue lines) ITD discretizations and the observed SIC in HadISST (dotted lines), NSIDC (dashed lines), and OSISAF (solid lines), in JFM (top) and ASO (bottom). Also, IIEE is shown between OSI SAF and NSIDC SIC (gray crosses), NSIDC and HadISST SIC (gray pluses), and HadISST and OSI SAF SIC (gray asterisks). The IIEE is calculated as the integrated area where simulations and observations disagree on ice concentration above 15% [Goessling et al., 2016].

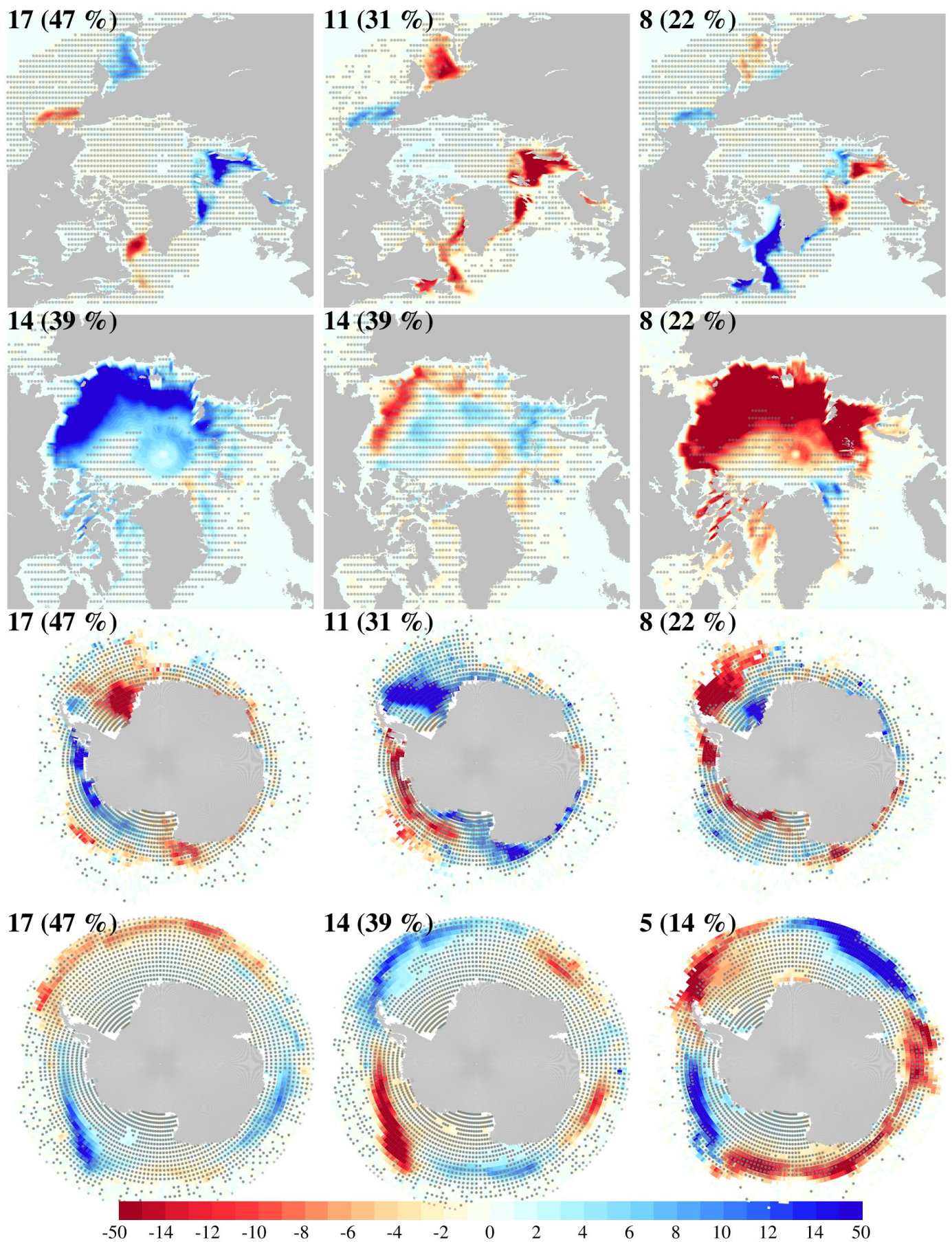


**Fig. S2:** Similar to Fig. 5 but for cluster patterns of Arctic (top two rows) and Antarctic (bottom two rows) SIC anomalies (shading; in % of area) in NSDIC in JFM (first and third rows) and ASO (second and fourth rows). The area is zoomed in over the Arctic in ASO (second row) for a better view of the central Arctic. Clusters are calculated from the full SIC field without detrending. Stippling masks statistically nonsignificant anomalies at the 5% level. The shading color scale of the SIC anomalies is adapted for a better view of values in the range  $\pm 15$ .

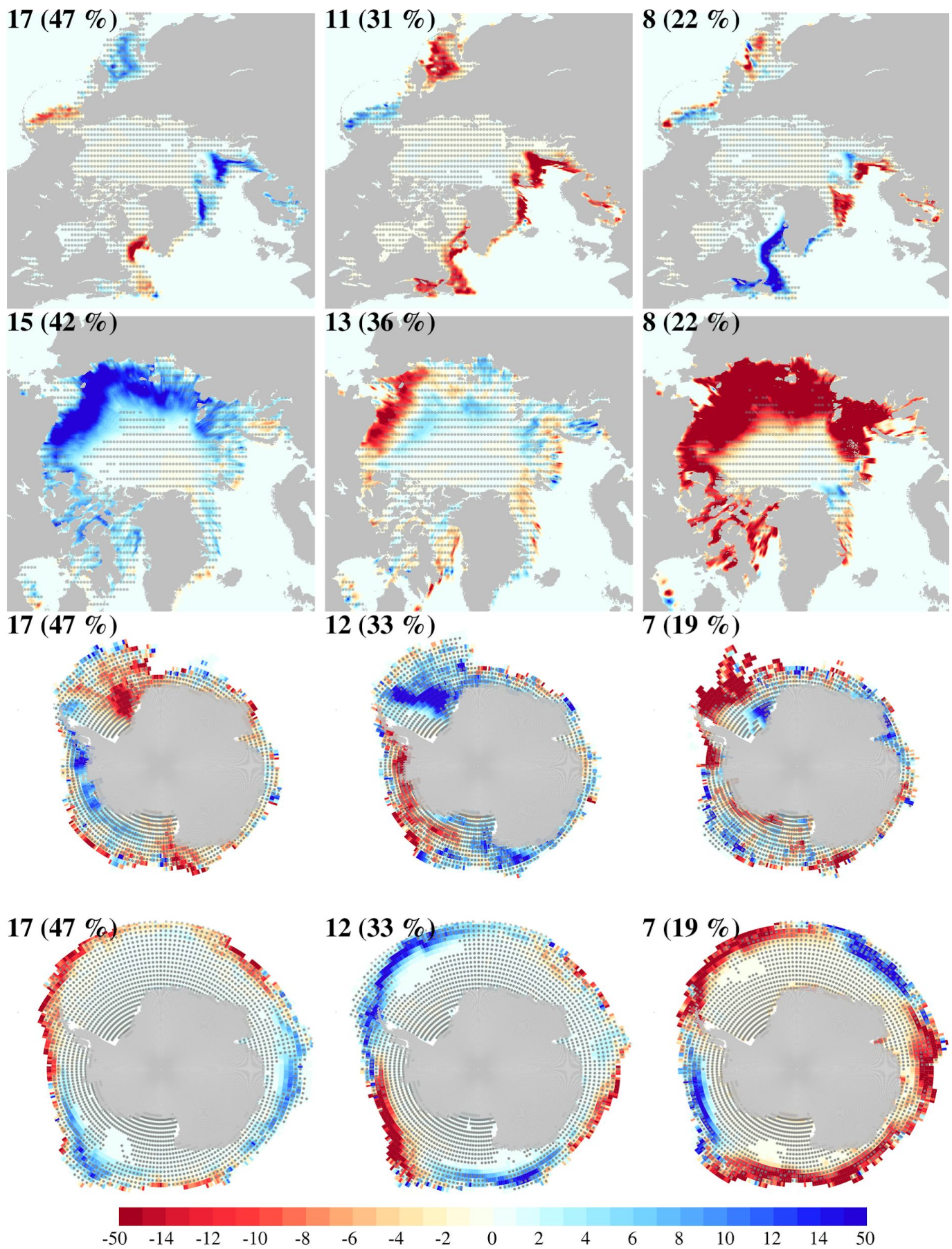


**Fig. S3:** As in Fig. S2 but for HadISST.

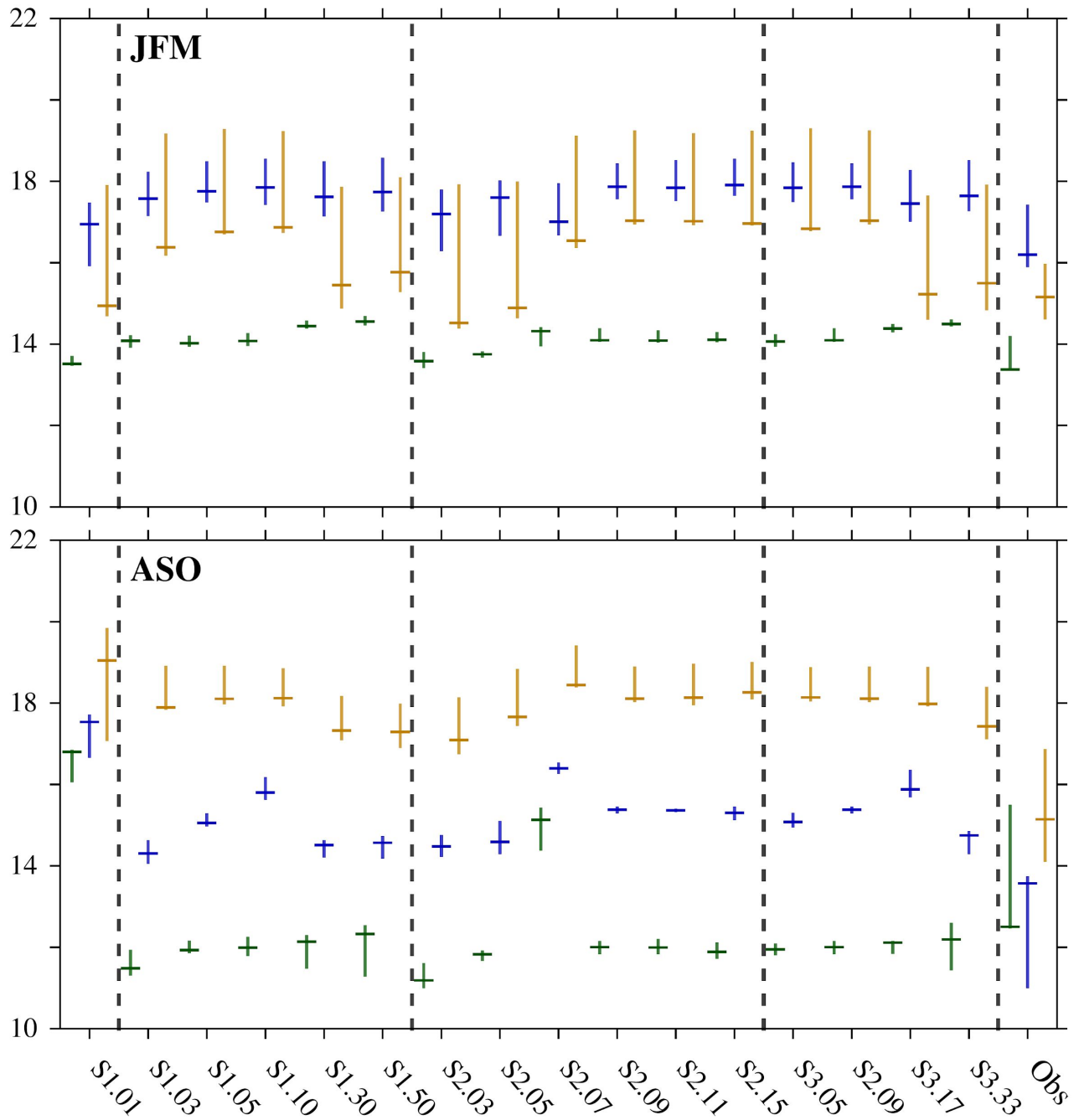


**Fig. S4:** Boxplot of the root-mean-square error (in % of area) between the simulated and observed clusters and across the three satellite observational products of Arctic SIC in JFM (top) and ASO (bottom). Results for the first, second, and third clusters are in green, blue, and orange, respectively. For each ITD discretization, three values are calculated with OSI SAF, NSIDC, and HadISST.

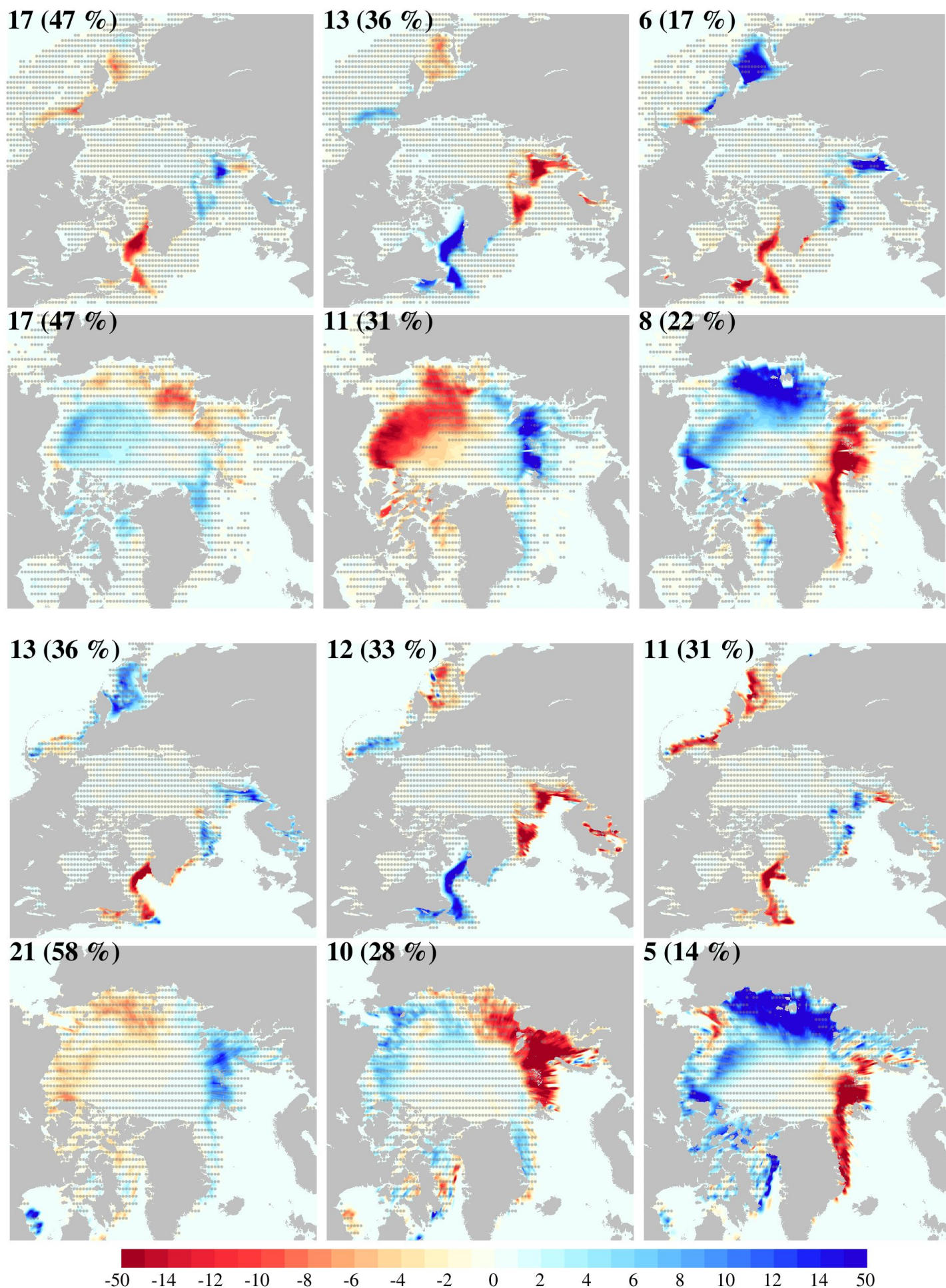


**Fig. S5:** As in Fig. S2 but for NSIDC and HadISST data (top and bottom two rows, respectively) after detrending with a second-degree polynomial and in the Arctic only.

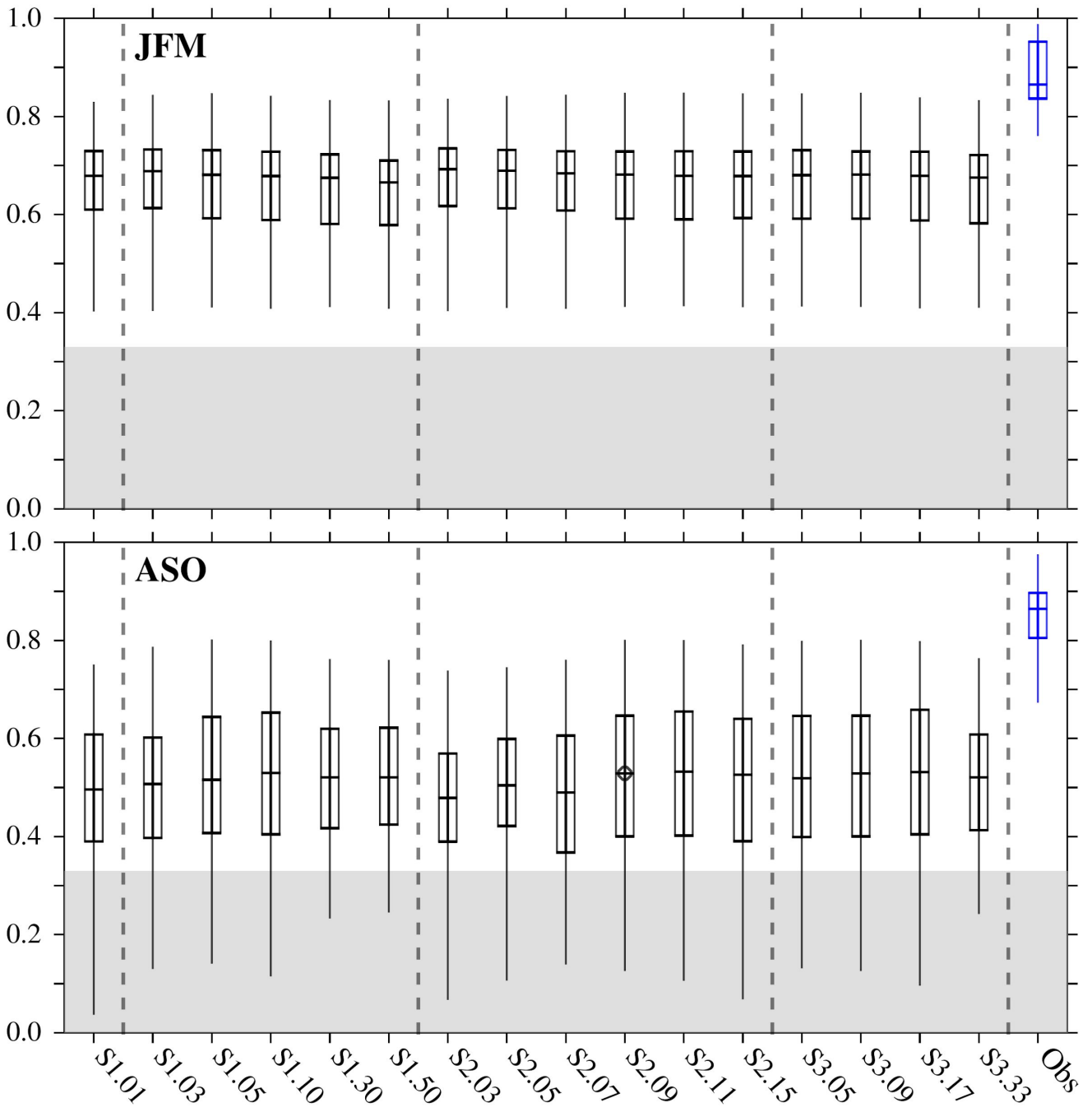


**Fig. S6:** Boxplot of spatial correlation coefficients between the simulated and observed anomaly fields (gray) and across the three satellite observational products (blue) of Arctic SIC in JFM (top) and ASO (bottom) between 1979 and 2014. For each ITD discretization, a distribution of 36 spatial correlation coefficients, corresponding to 36 years, is computed from the spatial correlation coefficients between its anomalies and those in OSISAF, NSIDC, and HadISST. Similarly, three 36-coefficient distributions are obtained between the three observational products. From these distributions, the maximum and minimum values, the 25th, 50th (median), and 75th percentiles are calculated and plotted. A dot is plotted when the difference between the median correlation coefficient values in one discretization and the one immediately below within the same discretization type is statistically significant, based on Fisher's  $z$  transform assuming a two-tailed 5% level. Gray shading masks statistically nonsignificant coefficients below 0.39 value, which corresponds with the minimum value across all the computations that are statistically significant at the 5% level, accounting for effective degrees of freedom and spatial autocorrelation. Dashed vertical lines separate between results in the simulation with one category (S1.01), in the different ITD discretizations (S1, S2, and S3), and in the observations.

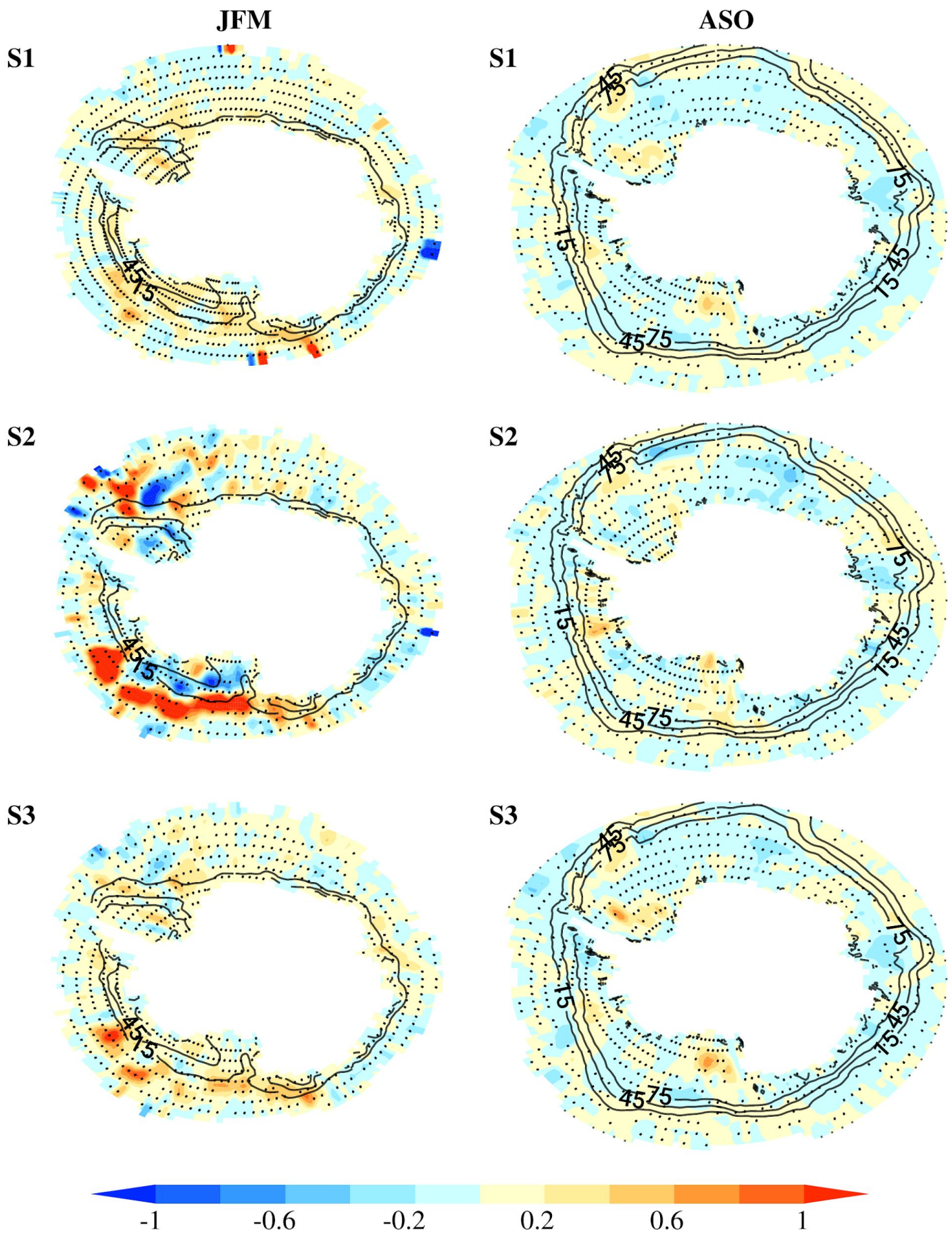


**Fig. S7:** As in Fig. 11, but for in Antarctica. Contours are climatological SIC for the period 1979–2014 in OSI SAF.